HHS Public Access

Author manuscript

Nat Neurosci. Author manuscript; available in PMC 2012 June 01.

Published in final edited form as:

Nat Neurosci. ; 14(12): 1574–1580. doi:10.1038/nn.2958.

Orientation Tuning of Cytochrome Oxidase Patches in Macaque Primary Visual Cortex

John R. Economides[1,*], **Lawrence C. Sincich**[2,*], **Daniel L. Adams**[1], and **Jonathan C. Horton**[1]

[1]Beckman Vision Center, University of California, San Francisco, San Francisco, CA 94143 USA

[2]Department of Vision Sciences, School of Optometry, University of Alabama at Birmingham, Birmingham, Alabama

Abstract

The abundant concentration of cytochrome oxidase in patches or blobs of primate striate cortex has never been explained. Patches are thought to contain unoriented, color-opponent neurons. Lacking orientation selectivity, these cells might endow patches with a high level of metabolic activity because they respond to all contours in visual scenes. To test this idea, orientation tuning was measured in layer 2/3 of macaque V1 using acutely implanted 100-electrode arrays. Each electrode recording site was identified, and assigned to the patch or interpatch compartment. The mean orientation bandwidth of cells was 28.4° in patches and 25.8° in interpatches. Neurons in patches were indeed less orientation selective, but the difference was subtle, indicating that the processing of form and color is not strictly segregated in V1. The most conspicuous finding was that patch cells had a 49% greater overall firing rate. This global difference in neuronal responsiveness, rather than an absence of orientation tuning, may account for the rich mitochondrial enzyme activity that defines patches.

Introduction

In patients with lesions of the fusiform gyrus the perception of color is abolished, although the ability to detect form remains intact[1]. It is unclear where the pathways which serve color and form begin to diverge in the visual system. In the retina, most ganglion cells do double duty, conveying information about both form and color. Once their signals have been filtered by the lateral geniculate nucleus and reach the primary visual cortex (striate cortex, V1), are the sensations of form and color mediated by separate populations of cells?

There are two compartments in the primary visual cortex, divided by the distribution of a mitochrondrial enzyme, cytochrome oxidase (CO). Histochemical staining for the enzyme reveals a regular pattern of dark patches (“blobs”, “puffs”), surrounded by paler tissue[2, 3].

Corresponding author: Jonathan C. Horton MD PhD, Beckman Vision Center, University of California, San Francisco, hortonj@vision.ucsf.edu, 10 Koret Way, San Francisco, CA 94143-0730, Phone: 415-476-6057, Fax: 415-476-8309.

*These authors contributed equally.

Author Contributions

All authors participated in the physiological recording experiments, data analysis, and preparation of this paper.

Tangential microelectrode penetrations through striate cortex have shown that neurons within blobs do not show orientation selectivity, whereas cells between blobs are highly orientation-selective. In addition, blob cells have color-opponent receptive field properties. These two key findings – lack of orientation selectivity and color-opponency – have led to the view that in V1 "a system involved in the processing of color information, especially color-spatial interactions, runs parallel to and separate from the orientation-specific system"[4, p. 309]. This functional segregation could explain the dissociation of color and form perception in the visual system, but it has hinged on the considerable challenge of correlating the receptive field properties of individual cells with the location of CO patches in striate cortex[5].

Recently, 100-electrode arrays have become available for recording single cells in the cerebral cortex[6–9]. These devices permit one to carry out a quantitative assessment of any receptive field parameter for scores of cells simultaneously, eliminating the one-cell-at-a-time bottleneck of the single microelectrode. They also eliminate the need to extrapolate between lesions along a microelectrode trajectory to infer the position of recording sites. Each electrode in the array leaves a small defect, allowing one literally to pinpoint each V1 recording site with respect to the cortical layers and the CO patches. Although designed for chronic implantation in alert, behaving animals, multi-electrode arrays can be used for acute recordings[6]. Here, they have been employed to examine the orientation specificity of cells in macaque striate cortex, comparing the tuning of cells in CO patches versus interpatches.

Results

Alignment of Electrodes with Cytochrome Oxidase Patches

Electrode arrays were implanted in opercular V1, representing eccentricities between 2° – 8° (Supplemental Fig. 1). When most of the electrodes penetrated only the superficial cortical layers, the array footprint was not immediately obvious in histological sections (Fig. 1a). Nonetheless, all 100 holes could be located by searching carefully in tangential sections through layer 2/3 processed for CO activity (Fig. 1b). It was vital to be sure that each hole was truly from an electrode shaft, not a blood vessel. Occasional blood clots, caused by hemorrhage along the electrode shafts, and small clumps of red blood cells, were helpful for identifying electrode holes. In addition, electrode holes could be distinguished from blood vessels by noting their grid-like spacing, absence of bifurcations, lack of endothelium, and tendency to end in the same cortical layer as adjacent holes.

Our goal was to record from cells in layer 2/3, where patches have maximum contrast, to compare our results directly to those reported previously[4]. For this reason, it was crucial to figure out the layer in which each electrode tip ended. This was accomplished by systematically following each electrode hole from the pial surface, section by section through the cortex, until it disappeared (Fig. 2). Sometimes, the pneumatic device used to insert the array propelled the electrode tips more deeply than intended into the cortex. In these cases, the resulting 10 × 10 grid was easy to identify because the holes were large, owing to the fact that the electrodes become thicker at their base. Unfortunately, data from deep electrodes could not be used because our aim was to examine orientation tuning in layer 2/3 patches.

The boundaries of the patches were defined by thresholding CO activity in the deepest section through layer 3. A circle of 75 μm radius, representing the maximum distance over which an electrode would be likely to pick up action potentials from a cell, was centered on the hole left in the tissue by each electrode shaft[10]. For this array, at 42/61 sites the circle was located entirely within the territory of a patch or interpatch in layer 2/3 (Fig. 1b). In such cases, there was no doubt about the identity of cells recorded by the electrode. However, at 19 sites the circle crossed a patch/interpatch boundary. In this situation, the cells recorded by the electrode were designated as “patch” or “interpatch” based on the location of the center of the circle. Usually, the center pixel was relatively far from a patch boundary, so this approach classified most cells accurately. In a later analysis, we deal with the problem posed by electrodes which happened to straddle a patch boundary.

Recordings from Electrode Arrays

Immediately after electrode insertion, neurons had low firing rates and their extracellular potentials were small in amplitude, presumably from the trauma of driving the array into the cortex. Gradually the quality of recordings improved[6]. The recovery of cortical function was monitored at regular intervals by plotting the receptive fields of cells sampled on different electrodes. Once responses appeared robust, drifting achromatic sine wave gratings were presented on a computer monitor. To assess orientation tuning, the gratings were displayed for 2 sec epochs, randomly varying the orientation in 10° intervals. Data were obtained from 8 successful array insertions in 5 animals. From these 8 arrays, 596 distinct waveforms were recorded from 366 electrodes located in layer 2/3.

Recording electrodes landed by chance in patches or interpatches (Fig. 3a). On about half the electrodes, multiple distinct waveforms were observed. K-means cluster analysis was performed on the first 3 principal component coefficients (Fig. 3b). Because the clusters were not always perfectly segregated, it is possible that some waveforms were misassigned. To assess the error rate, a silhouette value was calculated, with negative values denoting a waveform potentially assigned to the wrong cluster (Fig. 3c)[11]. Less than 10% of the points in each cluster had a negative silhouette value. Average waveforms were derived from each cluster (Fig. 3d).

Firing rates as a function of the motion direction of the oriented grating were plotted for each distinct average waveform (Fig. 3e). When multiple waveforms were distinguished at a given electrode, they generally had a similar preferred orientation. However, they often varied considerably in the strength of orientation tuning. This property was defined using two different criteria: peak bandwidth and circular variance. Each measure provides useful information about a neuron’s orientation selectivity[12]. Bandwidth reflects how sharply the cell’s peak response is tuned, and essentially ignores responses to other orientations. Circular variance takes into account the entire tuning curve, reflecting not only the shape of the peak, but the firing rate at other orientations as well[13]. For these example recordings, circular variance ranged from 0.30 to 0.73 (0 = oriented, 1 = unoriented) and bandwidth ranged from 20° to 34°. To determine the impact of events potentially assigned to the wrong cluster, the tuning curves in this example were recompiled after eliminating all points with negative silhouette values. This precaution altered the values for circular variance and

bandwidth by less than 2%, suggesting that overlap of event clusters had only a modest effect on orientation tuning indices.

Orientation tuning curves were plotted for all the waveforms recorded by electrodes in layer 2/3. For the example array insertion (Fig. 1), 65 tips were located in layer 2/3. CO activity was obscured by local hemorrhage around 4 electrodes, so these sites were excluded from analysis. Only background noise was recorded at another 10 electrodes. Of the remaining 51 electrodes, 15 were situated in patches and 36 in interpatches. At first glance, the tuning curves show no striking difference between the orientation selectivity of neurons in patches versus interpatches (Fig. 4)

Orientation Tuning of Patches versus Interpatches

The population of neurons recorded in the upper layers exhibited a wide range in circular variance and bandwidth (Supplemental Fig. 2). For patch cells, the values for circular variance were mean 0.64 ± 0.19, median 0.66 (n = 177) (Fig. 5a). For interpatch cells, the mean was 0.54 ± 0.20, median 0.54 (n = 419). Overall, orientation tuning was weaker in patches than in interpatches ($p < 0.001$, Wilcoxon rank-sum test). This was true in 3 of 5 monkeys when analyzed individually ($p < 0.05$), with a non-significant trend in a fourth monkey. In one animal, the circular variance was equal for patch and interpatch cells.

For patch cells, the bandwidth of orientation tuning curves had a mean of 28.4° ± 11.7° and a median of 26.8°. For interpatch cells, the values were mean 25.8° ± 10.9°, median 23.5° (Fig. 5a). The bandwidth difference between these two populations was 2.6° ($p < 0.001$, Wilcoxon rank-sum test). Neurons in patches had wider orientation bandwidths in 4 of 5 individual monkeys, although this trend reached significance ($p < 0.05$) in only one animal.

To assess orientation tuning, drifting gratings were presented at 4 different spatial frequencies: 0.5, 1, 2, and 4 cycles/deg. The spatial frequency which produced maximal firing at a cell's preferred orientation was used to calculate circular variance and bandwidth. Interestingly, there was no significant difference ($p > 0.98$ Wilcoxon rank-sum) in the optimal spatial frequency for patch units (1.40 ± 0.68 cycles/deg) compared with interpatch units (1.42 ± 0.71 cycles/deg).

Single Unit Data

The electrode arrays yielded a mixture of multiple unit and single unit recordings. Multiple unit activity might provide an inaccurate, low measure of orientation tuning strength, by merging signals from an ensemble of well-tuned cells which prefer different orientations. For this reason, an analysis was performed on data gathered only from well-isolated, single units.

For the 596 recorded waveforms, signal-to-noise ratio (SNR), defined as peak to trough amplitude divided by twice the standard deviation[6], ranged from 1.3 to 11.0, with a mean of 2.89. The SNR of recordings with 100-electrode arrays is usually lower than those from conventional microelectrodes[6]. The lower SNR is due to the fact that array electrodes have relatively low impedance (mean 280 kΩ for the array in Fig. 4) and they cannot be advanced closer to cells to increase spike amplitude. Consequently, our data set included low-

amplitude, multiple unit recordings that would not have been collected had the recordings been done with mobile, high impedance electrodes.

A histogram of the SNR for our recordings had a two peaked distribution, with a local minima at 2.55 (Fig. 5b). This trough corresponded closely to the intersection between the SNR distributions for average waveforms with a unimodal versus bimodal morphology (Fig. 5b). Unimodal average waveforms usually represent composite multiple unit recordings, whereas bimodal waveforms are more likely to constitute single units[14–16].

Orientation selectivity was analyzed for all waveforms that met two criteria: bimodal morphology and SNR > 2.55 (Fig. 5c). This subset was considered separately because it was likely to consist predominately of single units. For patches (n = 85) the mean circular variance was 0.65 ± 0.21 (median 0.69). For interpatches (n = 197) the mean circular variance was 0.53 ± 0.20 (median 0.53). For patches the mean bandwidth was 29.1° ± 12.1° (median 27.0°). For interpatches, it was 24.9° ± 11.6° (median 22.1°). For both measures of orientation selectivity, cells in patches were more broadly tuned than those in interpatches ($p < 0.001$, Wilcoxon rank-sum test). The elimination of low SNR and unimodal waveforms made no significant difference in the mean or distribution of circular variance and orientation bandwidth. This implies that SNR and orientation selectivity are not related. Indeed, plots of waveform SNR versus circular variance and bandwidth showed no correlation (Supplemental Fig. 3).

Correlation of CO Density with Orientation Selectivity

In histological sections processed for CO activity, the darkest 33% of striate cortex is commonly designated as patches[17, 18]. However, the exact percentage chosen to define patch boundaries is arbitrary. As mentioned earlier, the division of V1 into just two zones could misclassify cells recorded by electrodes located near the borders of patches. In addition, dichotomizing the cortex into two compartments might miss subtle trends in the spatial layout of oriented cells. For these reasons, circular variance and orientation bandwidth were plotted as continuous functions of CO density (Fig. 6). Scatter plots confirmed that neurons with broader orientation tuning tended to be located in regions of darker CO activity. The correlation was weak, and remained weak even when just single units (bimodal and SNR > 2.55) were considered. This analysis shows that changing the proportion of cortical territory assigned to patches does not alter the basic finding in this study.

Mean Population Tuning Curves

To compare the firing activity of cells recorded in patches (n = 177) versus interpatches (n = 419), the Gaussian fits for the largest peak of each neuron's orientation tuning curve were averaged to generate mean tuning curves (Fig. 7). These showed a 2.3° greater bandwidth for patch cells.

At the peaks, the firing rate was greater for patch cells (patch mean 13.2 ± 11.9 spikes/s; interpatch mean 10.7 ± 10.6 spikes/s, $p < 0.01$ Wilcoxon rank-sum test). However, when the offsets were taken into account, the peak amplitude of the response to visual stimulation was similar (patch mean 10.0 ± 9.6 spikes/s; interpatch mean 9.0 ± 9.8 spikes/s, $p = 0.28$ Wilcoxon rank-sum test). The greater offset for patch cells was due to a stronger response to

contours orthogonal to the optimal orientation (3.2 ± 4.2 spikes/sec versus 1.7 ± 1.9 spikes/sec, $p < 0.001$ Wilcoxon rank-sum test). The spontaneous activity, measured in the dark with no visual stimulation, was also slightly but significantly ($p < 0.002$ Wilcoxon rank-sum test) greater for patch cells (mean 1.2 ± 1.8 spikes/s) compared with interpatch cells (mean 0.9 ± 1.6 spikes/s).

The area under each mean tuning curve represents the overall firing rate for each population of cells. The integrated area was 49% greater for patch cells compared with interpatch cells. This marked difference in physiological activity during visual stimulation may explain, in part, the stronger CO activity present in patches.

These population mean tuning curves were compiled using the grating which yielded the maximum peak discharge rate (patch mean 1.40 cycles/deg; interpatch mean 1.42 cycles deg). Even at the lowest spatial frequency tested (0.5 cycles/deg), the peak firing rate was significantly greater ($p < 0.01$) for patch cells (mean 8.1 ± 9.6 spikes/s) compared with interpatch cells (mean 6.1 ± 7.0 spikes/s). It did not appear that at a lower spatial frequency than optimal, responses of interpatch cells were attenuated more than those of patch cells.

Discussion

The orientation tuning of cells was analyzed quantitatively by several investigators[19–22], following the original report that selectivity is sharply diminished in CO patches of macaque striate cortex[4]. In these subsequent studies, no relationship was found between the degree of orientation tuning and the density of CO staining in the upper layers. However, different primate species were examined, or histological sections were not cut parallel to the pial surface to reveal the two-dimensional layout of CO patches. It is difficult to delineate patches in sections cut perpendicularly or obliquely to the cortical surface, and even more difficult to achieve reliable alignment with fragments of electrode tracks marked by occasional lesions in serial sections. For these reasons, the orientation tuning of patch cells in macaque striate cortex has remained an unresolved issue, although these curious structures were discovered more than a quarter century ago[2, 3].

The 100-electrode arrays were designed for chronic implantation in alert animals[9]. No prior study has described the appearance of the array footprint post-mortem in cortical tissue. A major advantage of the arrays for acute physiological studies is that for each electrode one can identify reliably the layer in which it terminates and establish precisely the correlation with CO patches. Our data confirm that patch cells are more broadly tuned for orientation than interpatch cells. However, the difference between the populations is exceedingly subtle; most cells in patches retain strong orientation selectivity (Fig. 7).

We harbored some doubts about the health of the cortex during our recordings, because transient depression of neural activity occurred after each array implantation and intracortical hemorrhage was usually present post-mortem (Fig. 1). Tissue damage is less critical when arrays are used for chronic recordings, because the cortex has more time to recover from the insult of electrode insertion. Several factors, however, suggested that the discrepancy between our findings and those reported originally[4] was not simply an artifact

of using electrode arrays rather than single microelectrodes. First, the values for circular variance and orientation bandwidth we obtained closely resembled published data obtained from V1 using single microelectrodes (Supplemental Fig. 2)[12, 19, 23]. Second, one would expect injury from array insertion to degrade receptive field properties and reduce orientation selectivity, not increase it. Third, although multi-units were recorded on many electrodes, such recordings could not generate well-tuned orientation curves if patch cells truly do lack orientation selectivity. Fourth, while it is true that cell isolation is generally inferior with electrode arrays compared with single microelectrodes, our findings held even after culling unimodal and low signal-to-noise units (Fig. 5c). This result was consistent with a report that the orientation tuning of multi-unit and single unit activity recorded from V1 with 100-electrode arrays is highly correlated[24].

Orientation columns in macaque striate cortex converge in regions known as singularities or pinwheels[25, 26]. Neuronal selectivity for orientation varies systematically according to local map structure. With 100-electrode arrays, it has been shown that cells near singularities are more broadly tuned for orientation than cells located in radiating iso-orientation domains[8]. If CO patches coincide with singularities, this could explain the modest reduction in orientation selectivity displayed by patch cells (Fig. 5). Unfortunately, the spatial relationship between pinwheels and patches has been hard to establish, because it is difficult to achieve secure alignment between intrinsic signal orientation maps and CO histology, or even to define the exact location of pinwheel centers[27–31]. If there is no systematic overlap, it is worth pointing out that optical imaging has not revealed any other zones in striate cortex which might correspond to clusters of poorly oriented cells[4].

Cells in patches send an exclusive projection to CO thin stripes in V2. Dual-retrograde tracer injections into adjacent thin and pale stripes have confirmed that projections from patches and interpatches to V2 are isolated strictly from one other[32, 33]. This anatomy hints powerfully that patches have a specialized function, distinct from interpatches. Given that patches receive a direct projection from blue-yellow koniocellular geniculate neurons, it is natural to postulate that they are dedicated to color processing. Single cell physiology and optical imaging have provided support for this idea[34–37]. However, the fact that a structure receives direct input from a class of color-coded cells does not mean that it constitutes a separate color system. Layer 4Cβ, for example, receives direct input from red-green parvocellular neurons, but it is not considered a structure devoted to color, rather than to form. A small population of unoriented cells is likely to exist in patches, fed by direct koniocellular input. These units may contribute to the slightly broader mean orientation tuning of patches. However, the majority of cells in patches are well tuned, presumably because their strongest source of input arises from intracortical projections which build orientation selectivity[38].

Previously, it was thought that V1 color cells have radially symmetric, unoriented receptive fields[4]. Patches were expected to contain unoriented cells, because they mediate color perception rather than edge detection. Subsequently, it has been learned that many neurons in V1 respond to both equiluminant color and luminance modulation, and that these color-luminance units are well oriented, with a mean circular variance of 0.40[39]. Numerous studies have confirmed that color-responsive cells in V1 can be orientation selective[22, 40, 41].

Even double-opponent cells, reportedly prevalent in patches[4], are tuned for orientation[42]. These observations suggest that there is no contradiction between the finding that patches retain orientation tuning and the idea that they are involved in color vision.

Several recent fMRI studies have shown that blood oxygen level-dependent signals in striate cortex can discriminate between stimuli that differ in color and orientation, indicating that orientation-selective chromatic mechanisms emerge early in the human visual system[43–45]. In one paradigm, subjects viewed gratings which alternated between red and green or between +45° and −45°[46]. In the “double-conjunction” condition, the stimulus alternated simultaneously in color and orientation. The voxels that were most informative for the double-conjunction condition were distinct from those that were most informative about switches in color and orientation alone. This result implies that V1 contains local groups of cells jointly sensitive to orientation and color, perhaps corresponding to CO patches.

Our recordings indicated that neurons in patches had a higher mean peak firing rate (13.2 spikes/s versus 10.7 spikes/s) in response to visual stimulation (Fig. 7). In addition, the response to the anti-preferred orientation was nearly twice as great (3.2 spikes/s versus 1.7 spikes/s). This difference in the offset of the tuning curves of patch cells contributed to their higher circular variance, but did not account entirely for their broader tuning, because their peak orientation bandwidths averaged 10% wider (28.4° versus 25.8°). It would be interesting to compare surround inhibition for cells in patches versus interpatches, to see if this property contributes to the offset in firing rates.

A previous report noted that spike rates recorded in patches are 33% greater than in interpatches, but the result did not reach statistical significance because a low number of neurons was sampled[47]. Our 100-electrode array recordings showed that patch cells have a 49% higher mean overall firing rate compared with interpatch cells. This probably explains in part the greater level of metabolic activity exhibited by patches when V1 is processed for CO histochemistry. It also explains a curious finding from early 2-deoxyglucose studies. Under a wide variety of stimulus conditions, 2-deoxglucose uptake was found to be greatest in patches[2, 48, 49]. This observation led directly to the idea that patches contain unoriented cells. It was hypothesized that they are more active metabolically because they respond equally to contours of all orientation[4]. It now appears that most patch cells are well-oriented, but simply have a higher intrinsic mean firing rate than interpatch cells, either under spontaneous conditions or when driven by visual activity.

Supplementary Material

Refer to Web version on PubMed Central for supplementary material.

Acknowledgments

This work was supported by grants EY10217 (J.C.H.), EY13676 (L.C.S.) and EY02162 (Beckman Vision Center) from the National Eye Institute and by Research to Prevent Blindness. The California Regional Primate Research Center is supported by NIH Base Grant RR00169. Christina M. Jocson provided technical assistance and Matthew Feusner assisted with computer programming.

References

1. Heywood CA, Kentridge RW. Achromatopsia, color vision, and cortex. Neurol Clin. 2003; 21:483–500. [PubMed: 12916488]
2. Horton JC, Hubel DH. Regular patchy distribution of cytochrome oxidase staining in primary visual cortex of macaque monkey. Nature. 1981; 292:762–764. [PubMed: 6267472]
3. Wong-Riley M, Carroll EW. Effect of impulse blockage on cytochrome oxidase activity in monkey visual system. Nature. 1984; 307:262–264. [PubMed: 6319997]
4. Livingstone MS, Hubel DH. Anatomy and physiology of a color system in the primate visual cortex. J Neurosci. 1984; 4:309–356. [PubMed: 6198495]
5. Martin KAC. From enzymes to perception: A bridge too far? Trends in Neuroscience. 1988; 11:380–387.
6. Kelly RC, et al. Comparison of recordings from microelectrode arrays and single electrodes in the visual cortex. J Neurosci. 2007; 27:261–264. [PubMed: 17215384]
7. Smith MA, Kohn A. Spatial and temporal scales of neuronal correlation in primary visual cortex. J Neurosci. 2008; 28:12591–12603. [PubMed: 19036953]
8. Nauhaus I, Benucci A, Carandini M, Ringach DL. Neuronal selectivity and local map structure in visual cortex. Neuron. 2008; 57:673–679. [PubMed: 18341988]
9. Nordhausen CT, Maynard EM, Normann RA. Single unit recording capabilities of a 100 microelectrode array. Brain Res. 1996; 726:129–140. [PubMed: 8836553]
10. Henze DA, et al. Intracellular features predicted by extracellular recordings in the hippocampus in vivo. J Neurophysiol. 2000; 84:390–400. [PubMed: 10899213]
11. Kaufman, L.; Rousseeuw, PJ. Finding groups in data: an introduction to cluster analysis. Wiley & Sons; New York: 1990.
12. Ringach DL, Shapley RM, Hawken MJ. Orientation selectivity in macaque V1: diversity and laminar dependence. J Neurosci. 2002; 22:5639–5651. [PubMed: 12097515]
13. Swindale NV. Orientation tuning curves: empirical description and estimation of parameters. Biol Cybern. 1998; 78:45–56. [PubMed: 9518026]
14. Eliades SJ, Wang X. Chronic multi-electrode neural recording in free-roaming monkeys. J Neurosci Methods. 2008; 172:201–214. [PubMed: 18572250]
15. Nordhausen CT, Rousche PJ, Normann RA. Optimizing recording capabilities of the Utah Intracortical Electrode Array. Brain Res. 1994; 637:27–36. [PubMed: 8180807]
16. Kim SJ, Manyam SC, Warren DJ, Normann RA. Electrophysiological mapping of cat primary auditory cortex with multielectrode arrays. Ann Biomed Eng. 2006; 34:300–309. [PubMed: 16496084]
17. Purves D, LaMantia A. Development of blobs in the visual cortex of macaques. J Comp Neurol. 1993; 334:169–175. [PubMed: 8366193]
18. Farias MF, Gattass R, Piñón MC, Ungerleider LG. Tangential distribution of cytochrome oxidase-rich blobs in the primary visual cortex of macaque monkeys. J Comp Neurol. 1997; 386:217–228. [PubMed: 9295148]
19. Leventhal AG, Thompson KG, Liu D, Zhou Y, Ault SJ. Concomitant sensitivity to orientation, direction, and color of cells in layers 2, 3 and 4 of monkey striate cortex. J Neurosci. 1995; 15:1808–1818. [PubMed: 7891136]
20. Lennie P, Krauskopf J, Sclar G. Chromatic mechanisms in striate cortex of macaque. J Neurosci. 1990; 10:649–669. [PubMed: 2303866]
21. O'Keefe LP, Levitt JB, Kiper DC, Shapley RM, Movshon JA. Functional organization of owl monkey lateral geniculate nucleus and visual cortex. J Neurophysiol. 1998; 80:594–609. [PubMed: 9705453]
22. Friedman HS, Zhou H, von der Heydt R. The coding of uniform colour figures in monkey visual cortex. The Journal of physiology. 2003; 548:593–613. [PubMed: 12611925]
23. Schiller PH, Finlay BL, Volman SF. Quantitative studies of single-cell properties in monkey striate cortex. II Orientation specificity and ocular dominance. J Neurophysiol. 1976; 39:1320–1333. [PubMed: 825622]

24. Nauhaus I, Ringach DL. Precise alignment of micromachined electrode arrays with V1 functional maps. J Neurophysiol. 2007; 97:3781–3789. [PubMed: 17344376]
25. Blasdel GG, Salama G. Voltage-sensitive dyes reveal a modular organization in monkey striate cortex. Nature. 1986; 321:579–585. [PubMed: 3713842]
26. Bonhoeffer T, Grinvald A. Iso-orientation domains in cat visual cortex are arranged in pinwheel-like patterns. Nature. 1991; 353:429–431. [PubMed: 1896085]
27. Polimeni JR, Granquist-Fraser D, Wood RJ, Schwartz EL. Physical limits to spatial resolution of optical recording: clarifying the spatial structure of cortical hypercolumns. Proc Natl Acad Sci U S A. 2005; 102:4158–4163. [PubMed: 15746240]
28. Blasdel GG. Orientation selectivity, preference, and continuity in monkey striate cortex. J Neurosci. 1992; 12:3139–3161. [PubMed: 1322982]
29. Bartfeld E, Grinvald A. Relationships between orientation-preference pinwheels, cytochrome oxidase blobs, and ocular-dominance columns in primate striate cortex. Proc Natl Acad Sci U S A. 1992; 89:11905–11909. [PubMed: 1465416]
30. Landisman CE, Ts'o DY. Color processing in macaque striate cortex: electrophysiological properties. J Neurophysiol. 2002; 87:3138–3151. [PubMed: 12037214]
31. Xu X, et al. Functional organization of visual cortex in the owl monkey. J Neurosci. 2004; 24:6237–6247. [PubMed: 15254078]
32. Sincich LC, Horton JC. Divided by cytochrome oxidase: a map of the projections from V1 to V2 in macaques. Science. 2002; 295:1734–1737. [PubMed: 11872845]
33. Sincich LC, Horton JC. Input to V2 thin stripes arises from V1 cytochrome oxidase patches. J Neurosci. 2005; 25:10087–10093. [PubMed: 16267215]
34. Ts'o DY, Gilbert CD. The organization of chromatic and spatial interactions in the primate striate cortex. J Neurosci. 1988; 8:1712–1727. [PubMed: 3367218]
35. Landisman CE, Ts'o DY. Color processing in macaque striate cortex: relationships to ocular dominance, cytochrome oxidase, and orientation. J Neurophysiol. 2002; 87:3126–3137. [PubMed: 12037213]
36. Lu HD, Roe AW. Functional organization of color domains in V1 and V2 of macaque monkey revealed by optical imaging. Cereb Cortex. 2008; 18:516–533. [PubMed: 17576751]
37. Chatterjee S, Callaway EM. Parallel colour-opponent pathways to primary visual cortex. Nature. 2003; 426:668–671. [PubMed: 14668866]
38. Sincich LC, Horton JC. The circuitry of V1 and V2: integration of color, form, and motion. Annu Rev Neurosci. 2005; 28:303–326. [PubMed: 16022598]
39. Johnson EN, Hawken MJ, Shapley R. The spatial transformation of color in the primary visual cortex of the macaque monkey. Nat Neurosci. 2001; 4:409–416. [PubMed: 11276232]
40. Yoshioka T, Dow BM. Color, orientation and cytochrome oxidase reactivity in areas V1, V2 and V4 of macaque monkey visual cortex. Behav Brain Res. 1996; 76:71–88. [PubMed: 8734044]
41. Horwitz GD, Chichilnisky EJ, Albright TD. Cone inputs to simple and complex cells in V1 of awake macaque. J Neurophysiol. 2007; 97:3070–3081. [PubMed: 17303812]
42. Johnson EN, Hawken MJ, Shapley R. The orientation selectivity of color-responsive neurons in macaque V1. J Neurosci. 2008; 28:8096–8106. [PubMed: 18685034]
43. Sumner P, Anderson EJ, Sylvester R, Haynes JD, Rees G. Combined orientation and colour information in human V1 for both L-M and S-cone chromatic axes. Neuroimage. 2008; 39:814–824. [PubMed: 17964188]
44. Engel SA. Adaptation of oriented and unoriented color-selective neurons in human visual areas. Neuron. 2005; 45:613–623. [PubMed: 15721246]
45. McDonald JS, Mannion DJ, Goddard E, Clifford CW. Orientation-selective chromatic mechanisms in human visual cortex. J Vis. 2010; 10:34. [PubMed: 21047766]
46. Seymour K, Clifford CW, Logothetis NK, Bartels A. Coding and binding of color and form in visual cortex. Cereb Cortex. 2010; 20:1946–1954. [PubMed: 20019147]
47. DeYoe EA, Trusk TC, Wong-Riley MT. Activity correlates of cytochrome oxidase-defined compartments in granular and supragranular layers of primary visual cortex of the macaque monkey. Vis Neurosci. 1995; 12:629–639. [PubMed: 8527365]

48. Kennedy C, Des Rosiers MH, Sakurada O. Metabolic mapping of the primary visual system of the monkey by means of the autoradiographic ^{14}[C] deoxyglucose technique. Proc Natl Acad Sci U S A. 1976; 73:4230. [PubMed: 825861]

49. Tootell RB, Hamilton SL, Silverman MS, Switkes E. Functional anatomy of macaque striate cortex. I Ocular dominance, binocular interactions, and baseline conditions. J Neurosci. 1988; 8:1500–1530. [PubMed: 3367209]

50. Horton JC. Cytochrome oxidase patches: a new cytoarchitectonic feature of monkey visual cortex. Philos Trans R Soc Lond B Biol Sci. 1984; 304:199–253. [PubMed: 6142484]

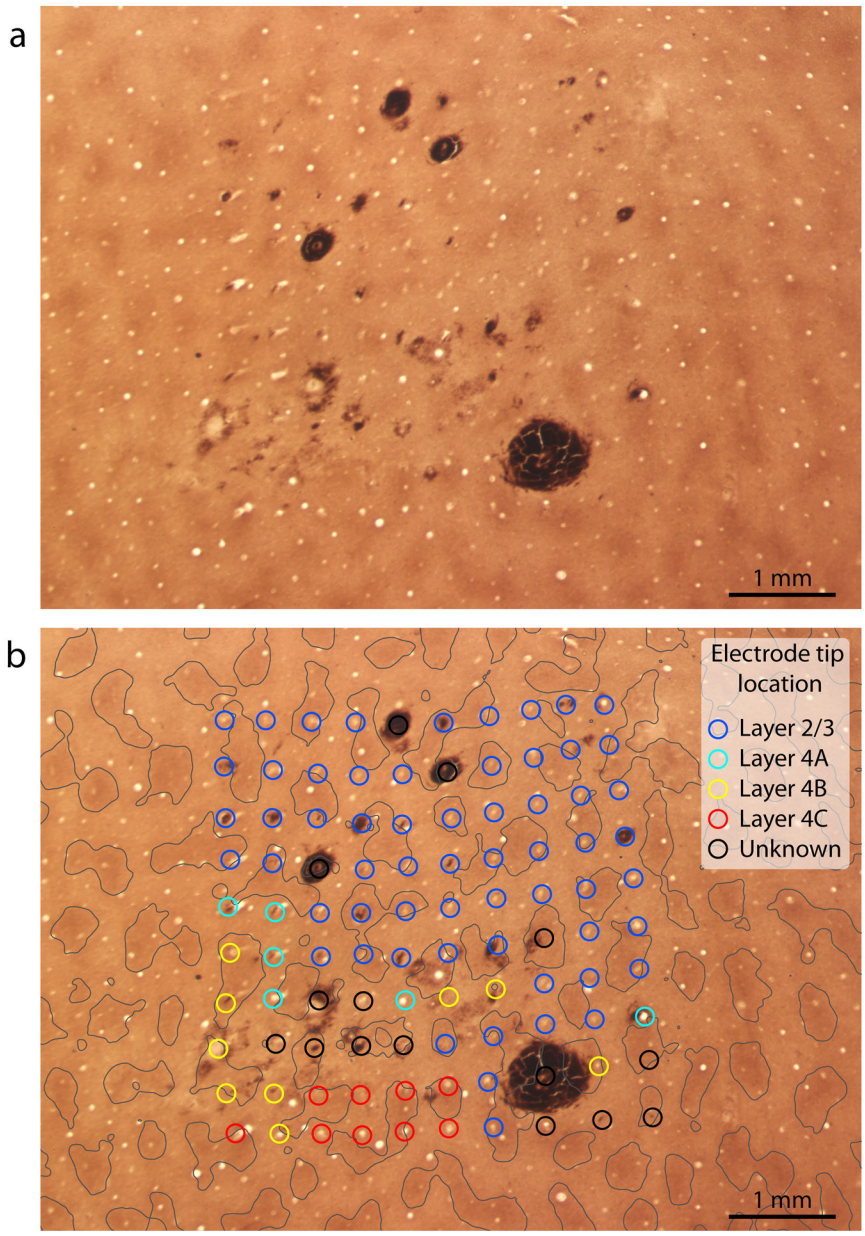

Fig. 1.

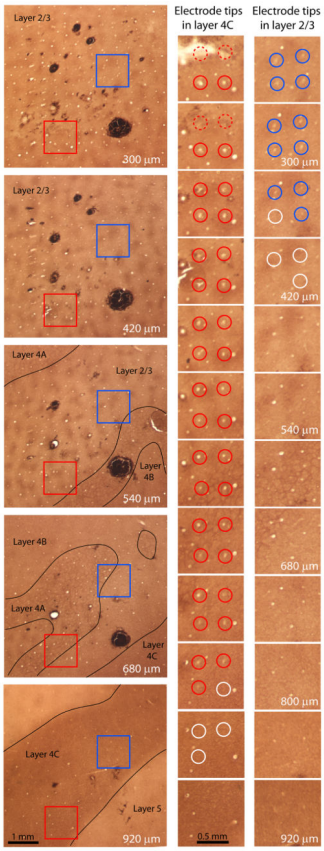

Fig. 2.

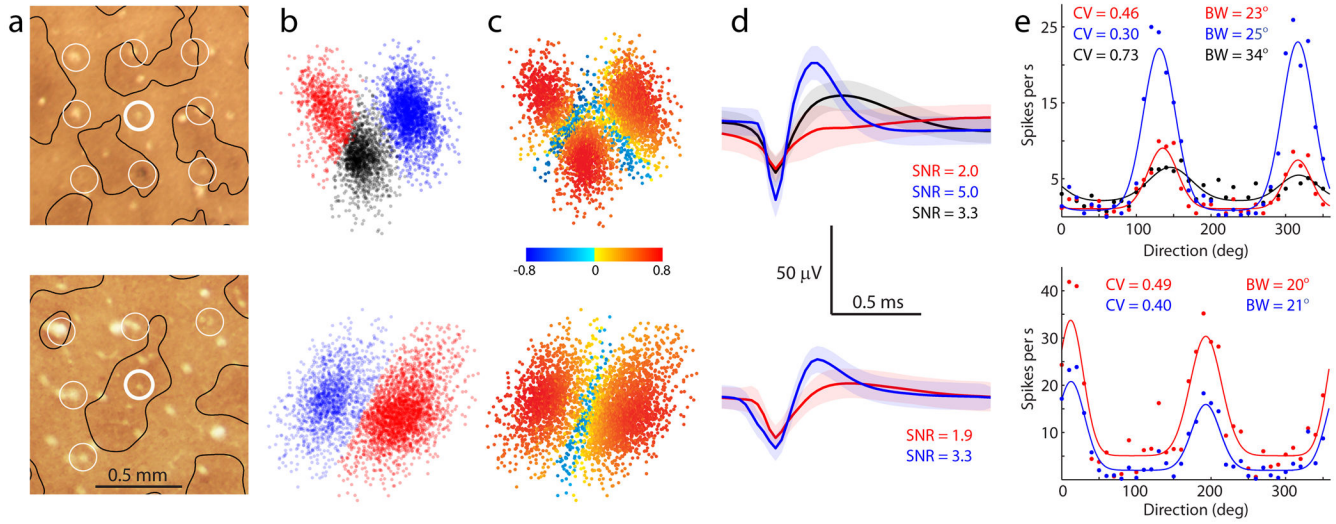

Fig. 3.

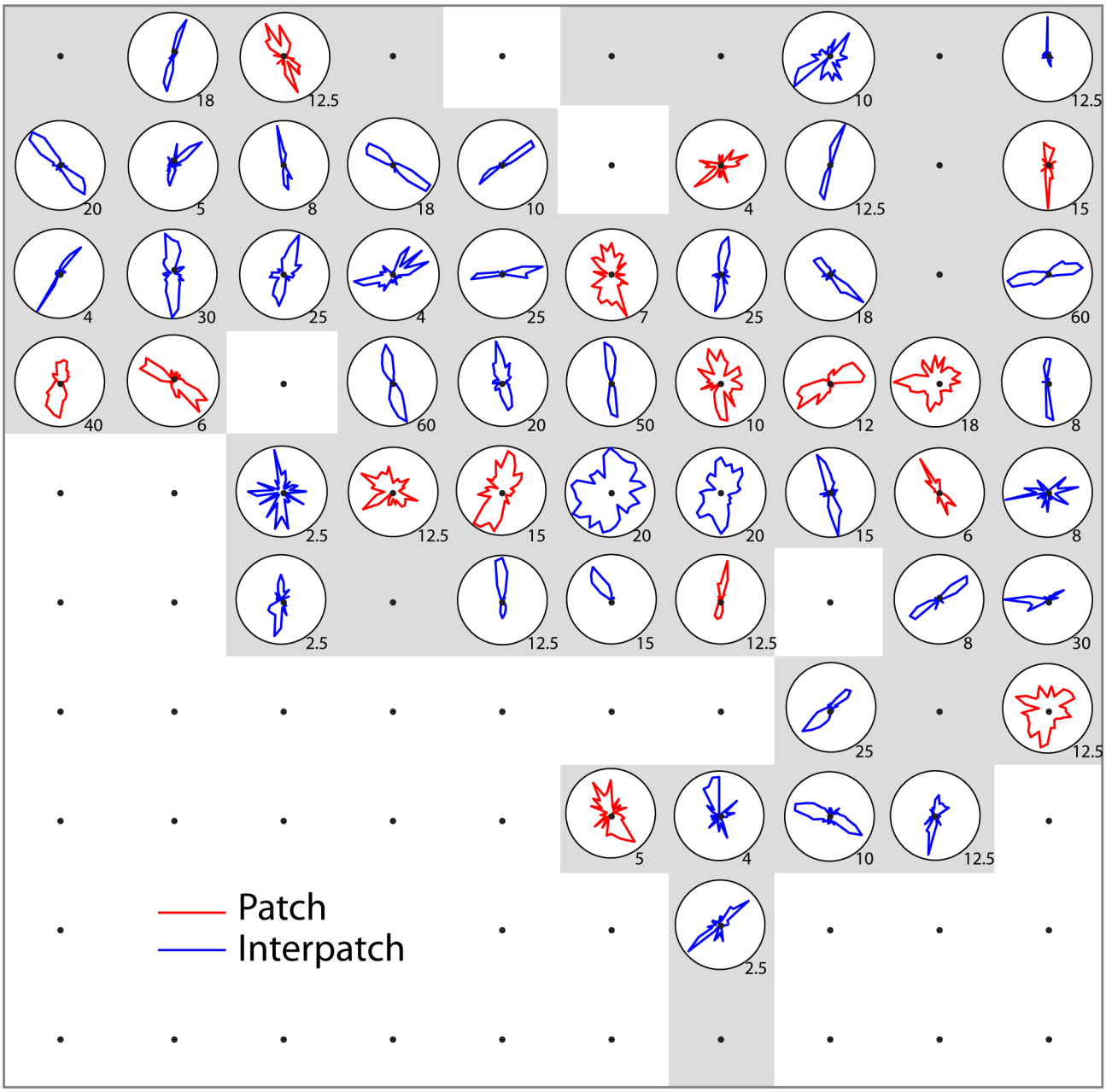

Fig. 4.

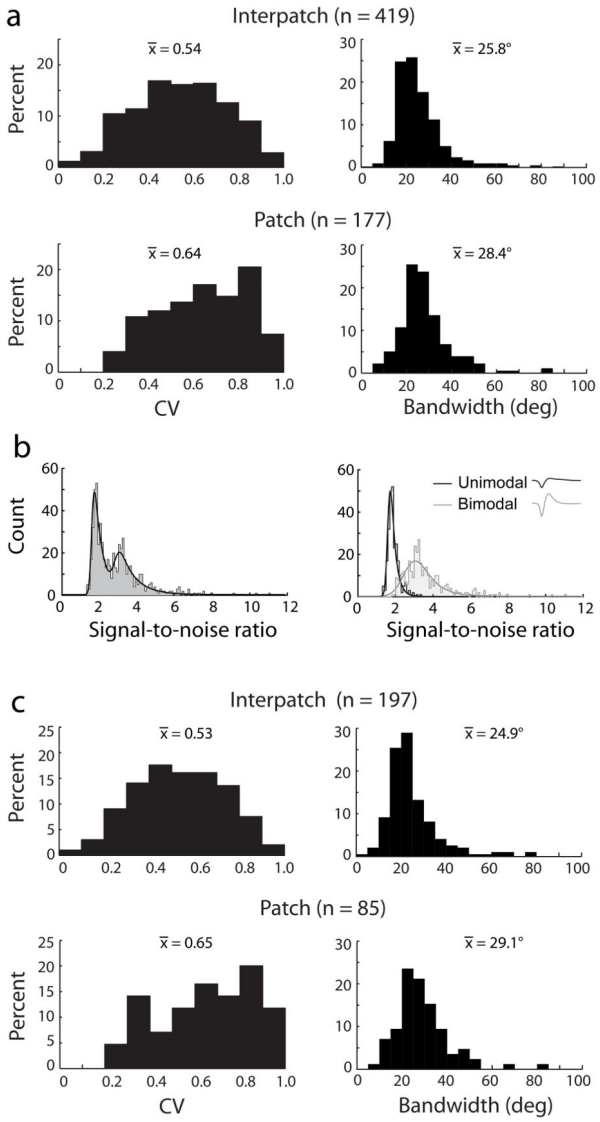

Fig. 5.

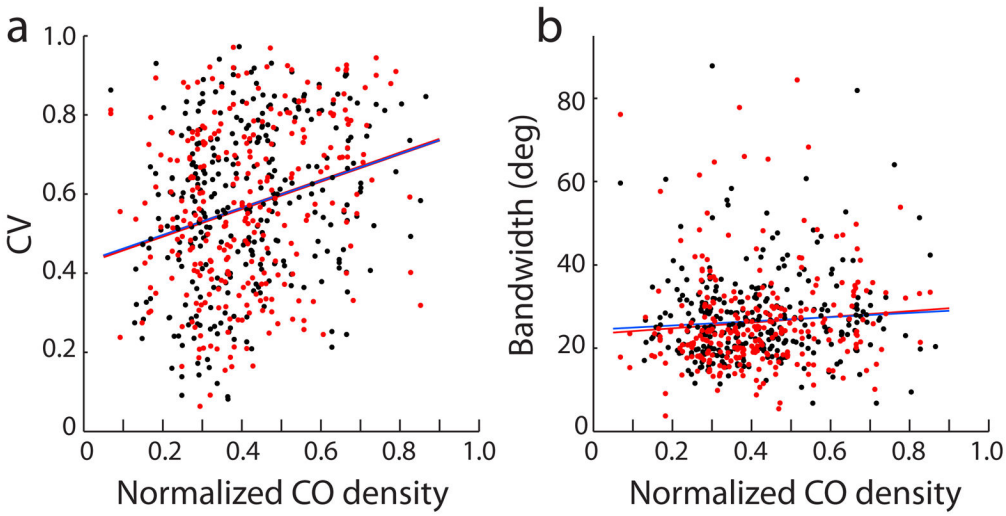

Fig. 6.

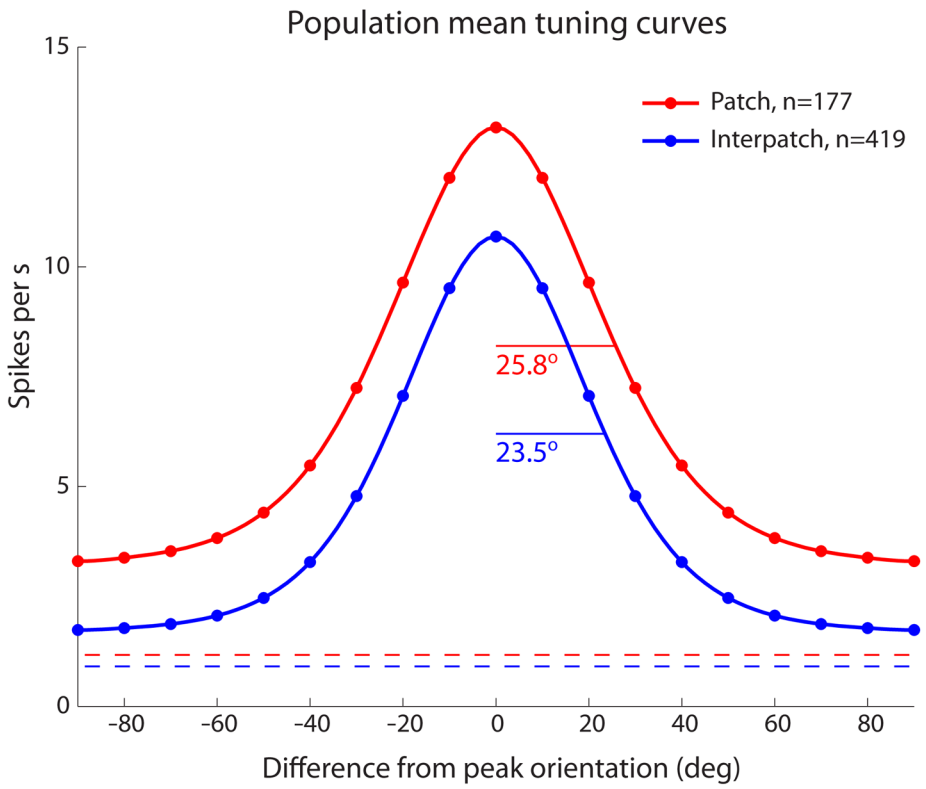

Fig. 7.